NASA Technical Memorandum 86759

On Blockage Corrections for Two-Dimensional Wind Tunnel Tests Using the Wall-Pressure Signature Method

S.R. Allmaras

(NASA-TM-86759) ON BLOCKAGE CORRECTIONS FOR TWO-DIMENSIONAL WIND TUNNEL TESTS USING THE WALL-PRESSURE SIGNATURE METHOD (NASA) 26 p
Avail: NTIS HC A03/MF A01 CSCL 01A

N87-27617

Unclas
G3/02 0091318

March 1986

LIBRARY COPY

MAR 17 1986

LANGLEY RESEARCH CENTER
LIBRARY, NASA
HAMPTON, VIRGINIA

National Aeronautics and
Space Administration

NASA Technical Memorandum 86759

On Blockage Corrections for Two-Dimensional Wind Tunnel Tests Using the Wall-Pressure Signature Method

S. R. Allmaras, Massachusetts Institute of Technology, Cambridge, Massachusetts

March 1986

NASA
National Aeronautics and
Space Administration

Ames Research Center
Moffett Field, California 94035

SYMBOLS

B	Tunnel width
b	Ratio of model chord to tunnel width (C/B)
C	Model chord
C_D	Sectional drag coefficient
C_p	Coefficient of pressure
c_s	Source/sink spacing distance
D	Sectional drag
Q	Source strength
q	Tunnel dynamic pressure $(\frac{1}{2}\rho u^2)$
U_∞	Freestream velocity
Δu	Perturbation velocity
Δx	Width at half height of symmetric signature
x	Axial spatial coordinate
y	Lateral spatial coordinate
ϵ	Centerline interference velocity; proportionality constant
ρ	Density

Subscripts:

B	Horizontal bouyancy
c	Corrected for blockage effects
m	Measured
p	Peak
s	Body/bubble (symmetric)
w	Wake (antisymmetric)
0	Origin
∞	Freestream

PRECEDING PAGE BLANK NOT FILMED

SUMMARY

The Wall-Pressure Signature Method for correcting low speed wind tunnel data to free-air conditions has been revised and improved for two-dimensional tests of bluff bodies. The method uses experimentally measured tunnel wall pressures to approximately reconstruct the flow field about the body with potential sources and sinks. With the use of these sources and sinks, the measured drag and tunnel dynamic pressure are corrected for blockage effects. Good agreement is obtained with simpler methods for cases in which the blockage corrections were about 10% of the nominal drag values.

INTRODUCTION

In recent wind tunnel tests of the downloads on the wings of the XV–15 Tilt-Rotor during take off and hover, large blockage effects were encountered (ref. 1). The validity of conventional theoretical blockage corrections used in the data reduction of these tests has not been established. As a result it was decided to use an alternative correction method, based more on experimental information, for a second series of tests. The chosen method, called the wall-pressure signature method, uses pressure distributions on the tunnel walls measured during the wind tunnel tests to better predict blockage corrections.

In the wall-pressure signature method the flow field about the body is approximated using the superposition of flows associated with a set of sources and sinks. The strengths and positions of these sources and sinks are determined so as to reconstruct the measured velocity distribution on the tunnel walls. Once determined the effect of the tunnel walls on the measured drag and dynamic pressure at the model is estimated and appropriate blockage corrections made.

The method was originally devised for three-dimensional (3–D) tunnel setups by Hackett, Wilsden, and Lilley (ref. 2) and has been revised for the two-dimensional (2–D) wind tunnel tests of the XV–15 wings.

The present report outlines the 2–D version of the wall-pressure signature method and gives a comparison between the blockage corrections obtained using this method and those of reference 1. In addition, descriptions of the programs used in the calculation of the blockage corrections are given in appendicies A, B and C.

WALL-PRESSURE SIGNATURE METHOD

Figure 1 shows a typical experimental setup for a 2-D wind tunnel. During the wind tunnel tests, the pressure distribution along the tunnel walls is one of the measurements recorded. This pressure distribution is converted to incremental or perturbation velocities about the freestream velocity (U_∞) by use of the definition of dynamic pressure

$$\frac{\Delta u}{U_\infty} = \sqrt{1 - \Delta C_p} - 1 \tag{1}$$

where ΔC_p is the net pressure coefficient after the wall pressure coefficients for the empty tunnel have been subtracted off.

The resulting incremental velocity distribution is assumed to consist of the superposition of the velocities for two flow fields, one symmetric and the other antisymmetric (fig. 2). The symmetric signature, modeling the body and its separation bubble, is constructed from a point source/sink pair ($\pm Q_s$) at a distance c_s apart. The antisymmetric signature, modeling the viscous wake of the body, is obtained from a single point source (Q_w) located at the peak of the symmetric velocity distribution.

I. Antisymmetric Signature Modeling (Wake)

For a point source of strength Q located at (x_0, y_0), the x-component of induced velocity at an arbitrary location (x, y) is given by

$$\Delta u = \frac{Q}{4\pi}\left[\frac{x - x_0}{(x - x_0)^2 + (y - y_0)^2}\right]. \tag{2}$$

Although the wake signature is modeled by a single source Q_w, a sink of equal strength at some downstream location must accompany it to ensure mass conservation. Further, the effects of the walls on the flow field can be simulated by the superposition of an infinite row of image systems as shown in figure 3. Thus, the velocity increment on one of the walls ($y = \pm B/2$), resulting from the wake source/sink pair, is

$$\left(\frac{\Delta u}{U_\infty}\right)_w = 2\left\{\frac{1}{4\pi}\left(\frac{Q}{U_\infty B}\right)\sum_{n=0}^{\infty}\left[\frac{\bar{x} - \bar{x}_2}{(\bar{x} - \bar{x}_2)^2 + (n + 1/2)^2} - \frac{\bar{x} - \bar{x}_5}{(\bar{x} - \bar{x}_5)^2 + (n + 1/2)^2}\right]\right\} \tag{3}$$

where the source is located at $(\bar{x}_2, 0)$ and the sink is located at $(\bar{x}_5, 0)$. The barred distances are nondimensionalized by the tunnel width B.

This equation is too cumbersome to calculate at each wall port location, especially considering that equation 3 is very slowly convergent. Hence, it will be approximated by a hyperbolic tangent function

$$\left(\frac{\Delta u}{U_\infty}\right)_w = A_1\left\{1 + \tanh\left[A_2(\bar{x} - \bar{x}_2)\right]\right\} \tag{4}$$

where the constants A_1 and A_2 are determined from numerical analysis of equation 3. Note that the downstream asymptote is $2A_1$ and the slope at $\bar{x} = \bar{x}_2$ is A_1A_2.

The downstream asymptote, taken to be the peak velocity at $\bar{x} = 1/2(\bar{x}_2 + \bar{x}_5)$, and the slope at $\bar{x}_2$ of equation 3 vary only slightly for the downstream sink located in the range $10 + \bar{x}_2 < \bar{x}_5 < 1000 + \bar{x}_2$. Using a large number of image systems ($\approx 50{,}000$), the summation terms (in braces) approach π and the slope at $\bar{x} = \bar{x}_2$ is 4.800. Thus the constants A_1 and A_2 become

$$A_1 = \frac{1}{4}\left(\frac{Q_w}{U_\infty B}\right), \qquad A_2 = 3.056. \tag{5}$$

In addition, since A_1 is half the asymptotic downstream velocity, the wake source strength is then given by

$$\frac{Q_w}{U_\infty B} = 2\left(\frac{\Delta u}{U_\infty}\right)_{x\to\infty} \tag{6}$$

Note that equation 6 is in conflict with the results of Hackett (ref. 2) by the factor of 2. The effect of this discrepency between the present analysis and that of Hackett's on the final blockage corrections is further detailed in section II of Results. Because of this discrepency a more detailed description of this analysis is also given in appendix D.

II. Symmetric Signature Modeling (Body/Bubble)

Once the wake signature is determined, it is subtracted from the measured wall velocities, leaving that portion due to the body/bubble. The resulting symmetric signature is curve fitted by a parabola

$$\left(\frac{\Delta u}{U_\infty}\right)_s = \alpha\bar{x}^2 + \beta\bar{x} + \gamma. \tag{7}$$

From this curve fit, the peak velocity and position are determined along with the width at half height. The data is filtered such that the points used for the curve fit properly model the upper half of the peak. From equation 7 these are given by

$$\text{Peak Velocity}: \quad (\Delta u/U_\infty)_{\max} = \gamma - \beta^2/4\alpha \tag{8}$$

$$\text{Peak Position}: \quad \bar{x}_p = -\beta/2\alpha \tag{9}$$

$$\text{Width at Half Height}: \quad \overline{\Delta x} = 2\sqrt{\frac{-(\Delta u/U_\infty)_{\max}}{2\alpha}}. \tag{10}$$

Once the parabola is determined, it becomes an inverse problem to find the source/sink strength and spacing which corresponds to that distribution. This task is accomplished by using $\bar{x}$ as input for two interpolation tables (appendix C). The output of these tables is the source/sink spacing

($\bar{c}_s$) and the maximum velocity normalized by source strength $(\Delta uB/Q_s)_{max}$, which is used with equation 8 to obtain the symmetric source/sink strength

$$\frac{Q_s}{U_\infty B} = \frac{(\Delta u/U_\infty)_{max}}{(\Delta uB/Q_s)_{max}}. \tag{11}$$

The source and sink positions are given by

$$\bar{x}_3 = \bar{x}_p - \frac{1}{2}\bar{c}_s, \qquad \bar{x}_4 = \bar{x}_p + \frac{1}{2}\bar{c}_s. \tag{12}$$

III. Iteration Procedure

Since the position of the wake source ($\bar{x}_2$) is not known prior to the use of equation 4, a value must first be assumed and then iterated upon.

Initially, the wake source position is assumed to be at the model location. The downstream asymptote is then determined from the data (see section I of Results), and the antisymmetric velocity distribution is calculated from equation 4. The result is subtracted off of the measured velocity distribution, and the resulting symmetric signature is curve fitted by the inverse parabola. If the peak position (eq. 9) is not sufficiently close to the assumed wake source position, a new value of $\bar{x}_p$ is chosen and the procedure is repeated until convergence is obtained.

Once this process is complete, the symmetric source/sink strengths and positions are obtained as outlined in section II, and the wake source strength is calculated by equation 6.

If the curve fit yields a divergent result, the symmetric signature is smoothed by replacing the value at each point by the average of the point and its two immediate neighbors. This averaging is done only once. If convergence is not obtained after the smoothing operation, the program defaults to a lower order linear theory, known as Hensel's method (ref. 3), to calculate the centerline interference velocity due to the symmetric signature.

IV. Centerline Interference Velocities

Once the source strengths and positions are known, the total centerline interference velocity distribution is obtained by superposing the effects of each of the three sources. For each source the interference velocity is found by using the position and strength as inputs for an interpolation table (appendix C).

As stated previously, if convergence cannot be obtained, the antisymmetric interference velocity is calculated as normal, but the symmetric signature contribution is obtained by Hensel's method (ref. 3). For 2-D source flow in a channel, Hensel's result is that for x-positions relatively close to the source position, the ratio of wall velocity to centerline interference velocity is simply 3.

V. Blockage Corrections for Dynamic Pressure and Drag

Given the interference velocity distribution along the tunnel centerline, the maximum velocity ($\epsilon_{\max}$) is found and used to correct the tunnel dynamic pressure

$$q_c = q_m(1 + \epsilon_{\max})^2 \tag{13}$$

where q_m is the measured tunnel dynamic pressure and q_c is the corrected dynamic pressure. Corrections to the measured drag coefficient include both effects of the tunnel q corrections and horizontal bouyancy.

In the original program of Hackett, horizontal bouyancy drag corrections were obtained by a method which uses the axial C_p gradient at the body. However, in the present test cases the axial extent of the model is not precisely known because of the high angles of attack. As a result it was decided that a second method should be used. This method, called the "ρuQ" method, recognizes from a momentum balance that the bouyancy drag on the model (ΔD_B) is given by

$$\Delta D_B = \rho(-\Delta u_s^+ Q_s + \Delta u_s^- Q_s - \Delta u_w^+ Q_w) \tag{14}$$

where $\Delta u^{\pm}$ is the induced velocity of each source. However, as mentioned before, a downstream wake sink is necessary for co tinuity; the drag of all four sources is then zero:

$$\Delta D_{\text{TOT}} = \rho(-\Delta u_s^+ Q_s + \Delta u_s^- Q_s - \Delta u_w^+ Q_w + \Delta u_w^- Q_w) = 0. \tag{15}$$

Thus, taking the difference between equations 14 and 15 gives

$$\Delta D_B = -\rho \Delta u_w^- Q_w. \tag{16}$$

Now, Δu_w^- is half the asymptotic velocity of the wake source which from equation 6 becomes

$$\Delta u_w^- = \frac{1}{4}\left(\frac{Q_w}{B}\right). \tag{17}$$

Then the drag coefficient correction for horizontal bouyancy is given by

$$\Delta C_{D_B} = -\frac{1}{2}\left(\frac{Q_w}{U_\infty B}\right)^2 \left(\frac{B}{C}\right) \tag{18}$$

where C is the model chord.

The total drag correction including dynamic pressure and bouyancy effects is

$$C_{D_c} = (C_{D_m} + \Delta C_{D_B})(q_m/q_c) \tag{19}$$

where C_{D_m} is the measured drag coefficient and C_{D_c} is the final, corrected drag coefficient.

VI. Reconstruction of Wall Velocities

Among the output from the program (appendix A) is a graphical comparison of the input tunnel wall velocities [illegible] calculated using the source/sink strengths and positions. This gives the user an indication of the accuracy that the tunnel wall velocities are reconstructed by the pressure-signature method. These reconstructed wall velocities are calculated in the following manner. Like the wake source (eq. 4) the effect of the symmetric source/sink pair is modeled by two hyperbolic tangent functions. The resulting reconstructed wall velocity signature is then given by

$$\frac{\Delta u}{U_\infty} = \frac{1}{4}\left(\frac{Q_w}{U_\infty B}\right)\left\{1+\tanh[A_2(\bar{x}-\bar{x}_2)]\right\} + \frac{1}{4}\left(\frac{Q_s}{U_\infty B}\right)\left\{\tanh[A_2(\bar{x}-\bar{x}_3)]-\tanh[A_2(\bar{x}-\bar{x}_4)]\right\}. \tag{20}$$

DISCUSSION OF RESULTS

I. Downstream Asymptotic Velocity

To calculate the antisymmetric velocity distribution, the asymptotic velocity is required. However, this value is not always accurately known because of such things as tunnel length restrictions and data spread. Thus, the sensitivity of the results to the choice of this asymptotic velocity must be investigated.

Figure 4 shows the measured pressure distribution for a test of the 30-cm triangle with apex forward (ref. 1). This case was analysed several times using different ports for the asymptotic velocity. The results, shown in table I, are typical of tests in this series.

As is shown in the table, the effect of the asymptote on the final dynamic pressure and drag corrections is small, even though there is a relatively large spread in the parameters of the individual sources (especially in their positions).

Using the search option of the program, the results would correspond to port 14 since it has the lowest velocity of the last few ports. Note also that the current version of the program will not use the last port as asymptote if the second to last port has a lower velocity.

II. Comparison with Hackett's Corrections

To see the effect of the discrepancy in equation 6 between Hackett's method and the present analysis on the final corrections, the aforementioned case was rerun using Hackett's version of

Table I: Comparison of Results Using Different Asymptotes

Port	$\%\Delta q^a$	$\%\Delta C_D{}^b$	$\epsilon_{\max}$	ΔC_{D_B}	Q_s/UB	Q_w/UB	$\bar{x}_2$	$\bar{c}_s$
11	5.60	−10.8	0.0275	−0.0923	0.0265	0.136	0.024	0.655
12[c]	5.69	−11.2	0.0282	−0.0969	0.0259	0.139	0.000	0.531
13[c]	5.79	−11.6	0.0287	−0.1014	0.0232	0.142	0.000	0.535
14	5.41	−10.2	0.0265	−0.0855	0.0291	0.131	0.065	0.715

[a]percent change in dynamic pressure $(q_c - q_m)/q_m$
[b]percent change in drag coefficient $(C_{D_c} - C_{D_m})/C_{D_m}$
[c]solution on verge of divergence

equation 6. Table II shows the comparison between the corrections for the two methods for the last entry in table I.

Table II: Comparison of Corrections for the Two Versions of Equation 6

Equation (6) Coefficient	$\%\Delta q$	$\%\Delta C_D$	$\epsilon_{\max}$	ΔC_{D_B}	Q_s/UB	Q_w/UB	$\bar{x}_2$	$\bar{c}_s$
2.0 (present)	5.41	−10.21	0.0265	−0.0855	0.0291	0.1307	0.065	0.715
1.0 (Hackett)	2.75	−5.28	0.0136	−0.0427	0.0291	0.0653	0.065	0.716

Table II shows that Hackett's corrections are approximately half of those using the present analysis of the wake strength to asymptotic velocity relationship.

III. Comparison with Conventional Blockage Corrections

As mentioned earlier, the reason for the present investigation was the uncertain validity of the conventional corrections used in reference 1 for the unusually large blockage effects found there. Here those corrections are compared with the present method for the triangle case of section I. In reference 1, the blockage correction formulas used were

$$q_c = q_m(1 + \epsilon b), \qquad C_{D_c} = C_{D_m}(1 - \epsilon b C_{D_m}) \tag{21}$$

where b is the ratio of model width to tunnel width, and ϵ was estimated to be 0.65 ± 0.05. For the triangle case of section I, $b = 0.10$ and the measured drag coefficient was $C_{D_m} = 1.582$. The corrections using these values are compared with those of the present method in table III.

The close comparison of the two methods shown in table III gives an indication that the corrections used in reference 1 were, in fact, valid despite the magnitude of the blockage effects.

Table III: Comparison with Convetional Blockage Corrections

Method	$\%\Delta q$	$\%\Delta C_D$
Pressure-Signature	5.41	-10.21
McCroskey (ref. 1)	6.50	-10.28
difference	1.11	0.07

CONCLUSIONS

The wall-pressure signature method for correcting low speed wind tunnel data to free-air conditions has been revised and improved for 2–D tests of bluff bodies. The method uses superposition of the flow fields associated with a set of three linear potential sources to approximate the flow about the body in the presence of the wind tunnel walls. Strengths and positions of the sources is determined so as to reconstruct the velocity distribution on the tunnel walls, which is obtained from measured pressure distributions taken during the wind tunnel tests of the model. With the use of these sources and sinks, the measured drag and tunnel dynamic pressure are then corrected for blockage effects.

This method has been used to apply blockage corrections of 2–D wind tunnel tests performed on the downloads on the wings of the XV–15 Tilt-Rotor during take off and hover. In these tests the blockage corrections were on the order of 10% of the measured drag values. The corrections obtained with this method were found to be in good agreement with the simpler methods used in reference 1.

APPENDIX A

MAIN PROGRAM DESCRIPTION: BLKAGE2D

The main blockage calculation program (BLKAGE2D) is a revised version of the 3–D code supplied by Hackett, Wilsden, and Lilley (ref. 2) for the CDC 7600 at NASA Ames Research Center.

The main operational difference between the two codes, other than conversion from 3–D to 2–D, is that if the symmetric signature cannot successfully be curve fitted, its points are smoothed. Then another curve fit is tried and if again unsuccessful, the program branches to Subroutine PUNT. In PUNT the wake, or antisymmetric portion, is kept and the symmetric portion is modeled by the Hensel computation. The impetus behind these changes is that it was found that for the present experiment, the wake signature alone fit the data well, leaving little more than experimental scatter for the symmetric portion in many cases.

Inputs

The program needs two separate inputs; the first is the individual run inputs and the second is the lookup charts.

Run Input (Sxxx.TMP)

Individual run input can again be broken down into two parts: main input, which is inputted once per run, and frame input for each frame of data. These two inputs have the following form. Unless otherwise specified, all input is in free format:

Main Input:

(1) RUNUM (A3)
(2) BTUN, CMOD, XMOD
(3) NWST, NBST
(4) XWST(I) I=1,NWST
(5) XBST(I) I=1,NBST
(6) LU, IUSES, IUSEE, ILIST, IDEBUG, ITAB
(7) IOPT

RUNUM = run number (3 digits)
BTUN = width of tunnel (ft)
CMOD = chord of model (ft)
XMOD = axial position of model (ft)
NWST = number of wall pressure ports
NBST = number of body pressure ports
XWST(I) = axial position of Ith wall port
XBST(I) = axial position of Ith body port
LU = plotter device number (=0)
IUSES = forward velocity asymptote
= 0 – zero asymptote
> 0 – velocity at IUSES port
IUSEE = aft velocity asymptote
= 0 – searches for smallest velocity after peak
< 0 – velocity at IUSEE port from end
> 0 – averages last IUSEE ports
ILIST = additional output option
= 0 – no added output
<> 0 – distripution of C_p and velocity along walls and C-L
IDEBUG = debugging output (no output if = 0)
ILAB = lookup charts output (no output if = 0)
IOPT = next input option
= 1 – new main input
= 0 – new frame input
=−1 – end

Frame Input:

(1) ALPHA
(2) CPWST(I) I=1,NWST
(3) CPEM(I) I=1,NWST
(4) CPB(I) I=1,NBST
(5) QU, PU
(6) CHDAT, CHTIM, CHILE, CHITE, CHVAR (2A8,3A15)
(7) IFRAME, CMUU, CLU, CDU, CMU
(8) IOPT

ALPHA = angle of attack (deg)
CPWST(I) = measured wall C_p at Ith port
CPEM(I) = empty tunnel wall C_p at Ith port
CPB(I) = measured body C_p at Ith body port
QU = measured dynamic pressure (psf)
PU = measured static pressure (psfa)
CHDAT = date of experiment (xx/xx/xx)
CHTIM = time of experiment (xx:xx:xx)
CHILE = description of leading edge
CHITE = description of trailing edge
CHVAR = variation description
IFRAME = frame number
CMUU,CDU,CLU,CMU = measured force coefficients (power, drag, lift, moment)

Charts Input (LOOKUP.TAB)

Lookup charts input is in the same form as output from LOOKUP:

(1) NDX, NX
(2) XDXOB(I) I=1,NDX
(3) CSOB(I) I=1,NDX
(4) XUFM(I) I=1,NDX
(5) XXOB(I) I=1,NX
(6) XUF(I) I=1,NX
(7) AT(I) I=1,3; AH(I) I=1,2

NDX = number of points in Charts I and II
NX = number of points in Chart III
XDXOB = width at half height
CSOB = source/sink spacing
XUFM = max velocity normalized by source strength
XXOB = axial position in tunnel
XUF = centerline interference velocity
AT = tanh constants (A_i in equations 4 and 20)
AT(1) = 3.056, AT(2)=AT(3)=0
AH = Hensel constants
AH(1) = 1/3, AH(2)=0

Output (Sxxx.OUT)

The program prints a main output (including a plot of measured and calculated wall velocities), along with three optional outputs depending on the values of ILIST, IDEBUG, and ITAB. In addition, a summary output is printed (Sxxx.SUM).

The following is a description of the output variables for each.

Output	Variable	Description
Main Output:		
EPS(MOD)	EPSMOD	C-L interference velocity at model
EPS(MAX)	EPSMAX	maximum C-L interference velocity (ϵ_{max})
X(MOD)/B	XMOD	axial position of model
X(MAX)/B	XP	axial position of peak symmetric velocity ($\bar{x}_2$)
XV/B	XVOB	axial position of wake source (Q_w)
BS/B	BSOB	not used in 2–D
DX/B	DXOB	width at half height
CS/B	CSOB1	source/sink spacing
QS/UB	QFS	solid body source strength (Q_s)
QW/UB	QFW	wake source strength (Q_w)
DCDWB	DCDW	bouyancy drag correction
US(MAX)/U	UOUMAX	maximum symmetric velocity on wall
UFM	UFMAX	maximum source-strength-normalized velocity
H FACTOR	HENSEL	ratio of peak symmetric wall velocity to maximum C-L interference velocity
A5	A5	half of asymptotic downstream velocity
A6	A6, AT(1)	tanh constant (λ_1 in eqs. 4 and 20)
A7	A7	not used in 2–D
Additional Output:		
X/B	XWST	axial position of wall ports
CP	CPWST-CPEM	measured zeroed C_p along wall
U/U	UOU	measured incremental velocity (plotted)
UA/U	UAOU	antisymmetric (wake) velocity along wall
US/U	USOU	symmetric (body/bubble) velocity along wall
UW/U	UWOU	computed wall velocity (plotted)
UP/U	UPOU	computed C-L interference velocity (body)
UV/U	UVOU	computed C-L interference velocity (wake)
EPS	SIGUOU	computed C-L interference velocity (total)
Lookup Chart Output:		
	– same as input format	
Debug Output:		
	– see code (Subroutine EPSCAL)	

APPENDIX B

AUXILIARY PROGRAMS DESCRIPTION

Two additional programs are needed for running BLKAGE2D. The first is a preprocessor, BLSETUP, and the second is a routine to setup the interpolation table for the empty tunnel wall pressure distribution.

Program BLSETUP

The main purpose of BLSETUP is to reduce wind tunnel data into pressure and force coefficients and then output the reduced data in a form which can be read in by BLKAGE2D.

The program is set up so that a subroutine reads in and reduces individual frames. This subroutine is taken from an off-line analysis routine called NEWA:

Inputs:	Sxxx.DAT	– wind tunnel data
	Syyy.EMP	– empty tunnel C_p interpolation table
Outputs:	Sxxx.TMP	– BLKAGE2D input

Program BLEMPT

Because the empty tunnel pressure distribution may change with tunnel dynamic pressure (i.e., Reynolds effects), Program BLKAGE2D was changed so that empty tunnel C_ps are read in for individual frames rather than once per run. Thus, BLSETUP must output empty tunnel C_ps which are appropriate for each frame's dynamic pressure. This task is accomplished by the use of an interpolation table in which tunnel q is the independent variable.

Program BLEMPT constructs this table. Since empty tunnel data is stored in the same format as normal runs, Program NEWA is again uses for data input and reduction.

After all frames of the empty tunnel run are input and reduced, the program prompts for which frames to average.

Inputs:	Syyy.DAT	– empty tunnel data
Outputs:	Syyy.EMP	– empty tunnel C_p interpolation table

It should be noted that the current versions of BLSETUP and BLEMPT disregard pressures from port 12 and replace them with the average of ports 11 and 13.

APPENDIX C

LOOKUP CHARTS

After the antisymmetric signature is subtracted from the measured wall velocity distribution, the resulting symmetric signature is curve fit by an inverted parabola. Then an inversion process is performed to obtain the source/sink strengths and positions which correspond to this parabolic distribution. This process is accomplished using interpolation tables (Charts I and II).

Further, after all source strengths and positions have been found, the centerline interference velocity must be found. This process also is accomplished by the use of an interpolation table (Chart III).

Charts I and II

Using the width at half height ($\overline{\Delta x}$) as input, Chart I outputs the source/sink spacing ($\bar{c}_s$), and Chart II outputs the maximum velocity normalized by the source strength $(\Delta uB/Q_s)_{\max}$.

Considering a source/sink pair located at $(0,0)$ and $(\bar{c}_s,0)$ in a tunnel (fig. 2), where the tunnel walls are simulated by a singly infinite row of image systems, the incremental velocity at a location on one of the walls ($y = \pm B/2$) is given by

$$\frac{\Delta u}{U_\infty} = \frac{1}{4\pi}\left(\frac{Q_s}{U_\infty B}\right)\sum_{n=-\infty}^{+\infty}\left[\frac{\bar{x}}{\bar{x}^2+(n+1/2)^2} - \frac{\bar{x}-\bar{c}_s}{(\bar{x}-\bar{c}_s)^2+(n+1/2)^2}\right]$$

or

$$\frac{\Delta uB}{Q_s} = \frac{1}{2\pi}\sum_{n=0}^{+\infty}\left[\frac{\bar{x}}{\bar{x}^2+(n+1/2)^2} - \frac{\bar{x}-\bar{c}_s}{(\bar{x}-\bar{c}_s)^2+(n+1/2)^2}\right] \tag{C1}$$

where barred distances are normalized by tunnel width B.

Charts I and II are constructed by the following procedure: For a given range of $\bar{c}_s$, the maximum source-strength-normalized incremental velocity ($\Delta uB/Q_s$) is determined by evaluating equation C1 at the midpoint $\bar{x} = \frac{1}{2}\bar{c}_s$. The width at half height is determined by iteration. This is done by evaluating equation C1 for different values of $\bar{x}$ until the position $\bar{x} = \bar{x}_{1/2}$ at which $\Delta uB/Q_s = 1/2(\Delta uB/Q_s)_{\max}$ is found. Then the width at half height is given by

$$\overline{\Delta x} = 2(\bar{x}_{1/2} - \frac{1}{2}\bar{c}_s). \tag{C2}$$

Chart III

Using $\bar{x}$ position as input, Chart III gives the centerline interference velocity (normalized by source strength) caused by the presence of tunnel walls on a single source of strength Q located on the centerline.

As in equation C1, the wall effects are simulated by a singly infinite row of image systems. However, in this case the equation is evaluated on the centerline ($y = 0$) and only the effects of the image systems are included.

$$\left(\frac{\Delta u}{U_\infty}\right)_{C-L} = \frac{1}{2\pi}\left(\frac{Q}{U_\infty B}\right)\sum_{n=1}^{+\infty}\left[\frac{\bar{x}-\bar{x}_0}{(\bar{x}-\bar{x}_0)^2+n^2}\right]. \tag{C3}$$

Chart III is constructed by evaluating equation C3 over a given range of $\bar{x}$ positions.

Program Description (LOOKUP)

The program used for construction of the lookup charts is called LOOKUP. Its inputs are as follows:

Charts I and II	–	(1) minimum and maximum values of $\bar{c}_s$
		(2) number of points in Chart I and II
Chart III	–	(3) minimum and maximum values of $\bar{x}$
		(4) number of points in Chart III
		(5) number of image systems used in calculation
		(6) iteration error parameter

It is suggested that a minimum value for $\bar{c}_s$ of not less than 0.05 be used. Also, since equations C1 and C3 are slowly convergent series, the number of image systems should be on the order of 10^5 or 10^6.

APPENDIX D

ANALYSIS OF WAKE VELOCITY APPROXIMATION

As stated in the text, there is a disagreement between Hackett's results and the present analysis in the relationship between the asymptotic velocity and the strength of the wake source. Therefore, it has been decided to detail the analysis of the wake velocity distribution and its approximation by a hyperbolic tangent function.

As stated in equation 3, the induced velocity distribution on the tunnel wall caused by the wake source/sink pair is given by

$$\left(\frac{\Delta u}{U_\infty}\right)_w = 2\left\{\frac{1}{4\pi}\left(\frac{Q_w}{U_\infty B}\right)\sum_{n=0}^{+\infty}\left[\frac{\bar{x}-\bar{x}_2}{(\bar{x}-\bar{x}_2)^2+(n+1/2)^2}+\frac{\bar{x}-\bar{x}_5}{(\bar{x}-\bar{x}_5)^2+(n+1/2)^2}\right]\right\} \qquad \text{(D1)}$$

where the factor of 2 comes from the fact that the summation terms account for the image systems on one side of the wall only (the influence of the images is symmetric about the wall).

Numerical experiments were run on the summation terms alone assuming the wake source to be at $\bar{x}_2 = 0$. Table D-I shows the results for the downstream asymptote and slope at $\bar{x} = \bar{x}_2$ for various sink locations ($\bar{x}_5$) and number of image systems used. The downstream asymptote is taken to be the peak velocity at the midpoint between the source and sink ($\bar{x} = \frac{1}{2}\bar{x}_5$).

Table D-I: Summation Terms for Asymptote and Slope

$\bar{x}_5$	Number of images	Asymptote	Slope @ $\bar{x}_2$
10	1,000	3.132	4.801
10	10,000	3.140	4.801
10	100,000	3.140	4.800
100	10,000	3.132	4.801
100	100,000	3.137	4.798
1000	10,000	3.133	4.801
1000	100,000	3.128	4.804

Table D-I shows that the asymptote and slope are nearly constant over a large range of sink locations and number of images used. From the table the asymptote can be taken as π and the slope at $\bar{x}_2$ as 4.800. This gives the asymptotic velocity

$$\left(\frac{\Delta u}{U_\infty}\right)_{x\to\infty} = \frac{1}{2\pi}\left(\frac{Q_w}{U_\infty B}\right)\left[\pi\right] = \frac{1}{2}\left(\frac{Q_w}{U_\infty B}\right) \qquad \text{(D2)}$$

and the slope at the source location

$$\frac{d}{dx}\left(\frac{\Delta u}{U_\infty}\right)\Big|_{x_2} = \frac{1}{2\pi}\left(\frac{Q_w}{U_\infty B}\right)\Big[4.800\Big] = \frac{2.4}{\pi}\left(\frac{Q_w}{U_\infty B}\right). \tag{D3}$$

The actual velocity distribution (eq. D1) is approximated by a hyperbolic tangent function as in equation 4.

$$\left(\frac{\Delta u}{U_\infty}\right)_w = A_1\Big\{1 + \tanh\left[A_2(\bar{x} - \bar{x}_2)\right]\Big\}. \tag{D4}$$

Noting that $\tanh(\bar{x}) \to 1$ as $\bar{x} \to \infty$, the asymptote of equation D4 is

$$\left(\frac{\Delta u}{U_\infty}\right)_{\bar{x}\to\infty} = 2A_1. \tag{D5}$$

The slope at $\bar{x} = \bar{x}_2$ is given by

$$\frac{d}{dx}\left(\frac{\Delta u}{U_\infty}\right)\Big|_{x_2} = A_1A_2\Big\{1 + \tanh\left[A_2(\bar{x} - \bar{x}_2)\right]\Big\}_{\bar{x}=\bar{x}_2} = A_1A_2. \tag{D6}$$

Thus, from equations D2 and D5, A_1 is given by

$$A_1 = \frac{1}{4}\left(\frac{Q_w}{U_\infty B}\right) \tag{D7}$$

and from equations D3, D6, and D7, A_2 becomes

$$A_2 = 3.056 \tag{D8}$$

REFERENCES

1. McCroskey, W. J.; Spalart, Ph.; Laub, G. H.; Maisel, M. D.; and Maskew, B.: Airloads on Bluff Bodies, with Application to the Rotor-Induced Downloads on Tilt-Rotor Aircraft. NASA TM–84401, 1983.

2. Hackett, J. E.; Wilsden, D. J.; Lilley, D. E.: Estimation of Tunnel Blockage from Wall Pressure Signatures: A Review and Data Correlation. NASA CR–15224, 1979.

3. Hensel, R. W.: Rectangular Wind Tunnel Blocking Corrections Using the Velocity-Ratio Method. NACA TN–2372, 1951.

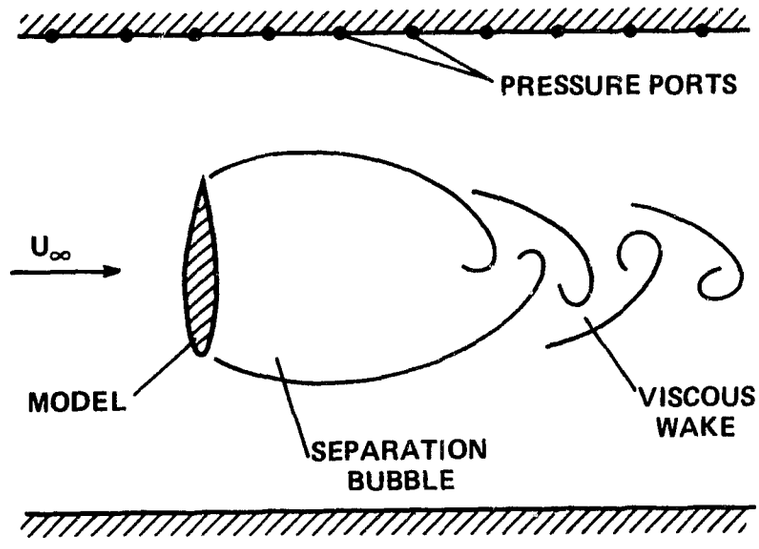

Figure 1. – Sketch of 2–D wing model in tunnel with wall pressure ports

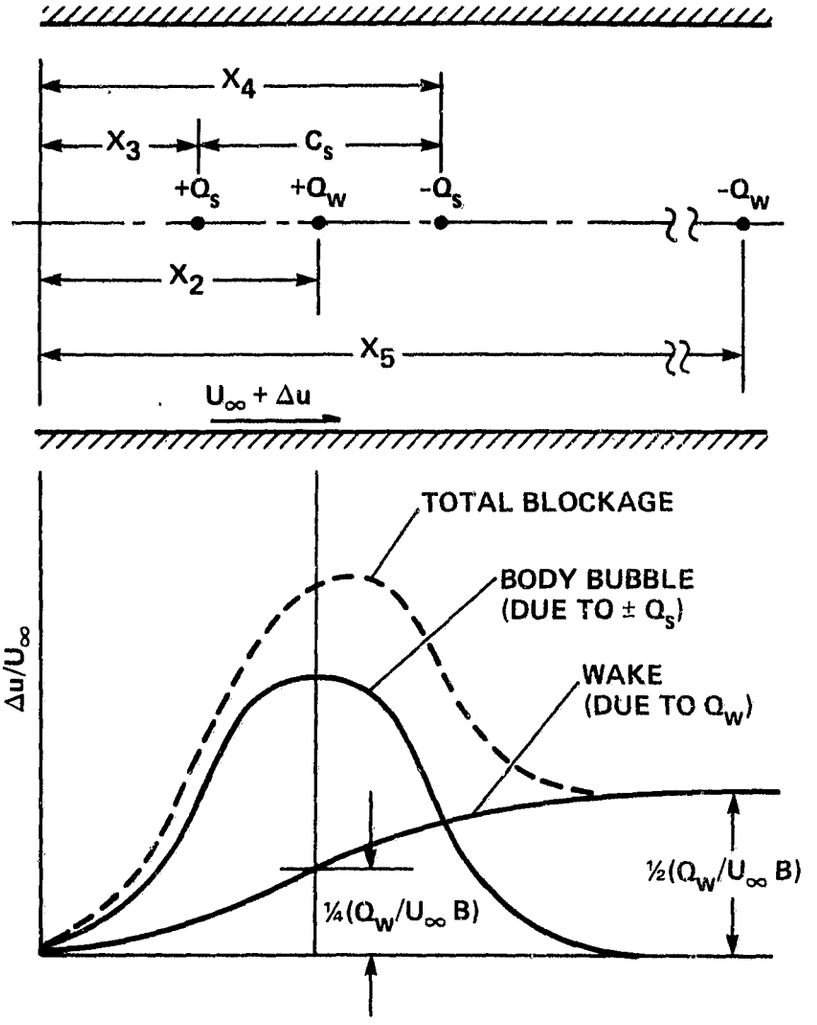

Figure 2. – Approximation to the flow field in the wind tunnel using potential sources and sinks

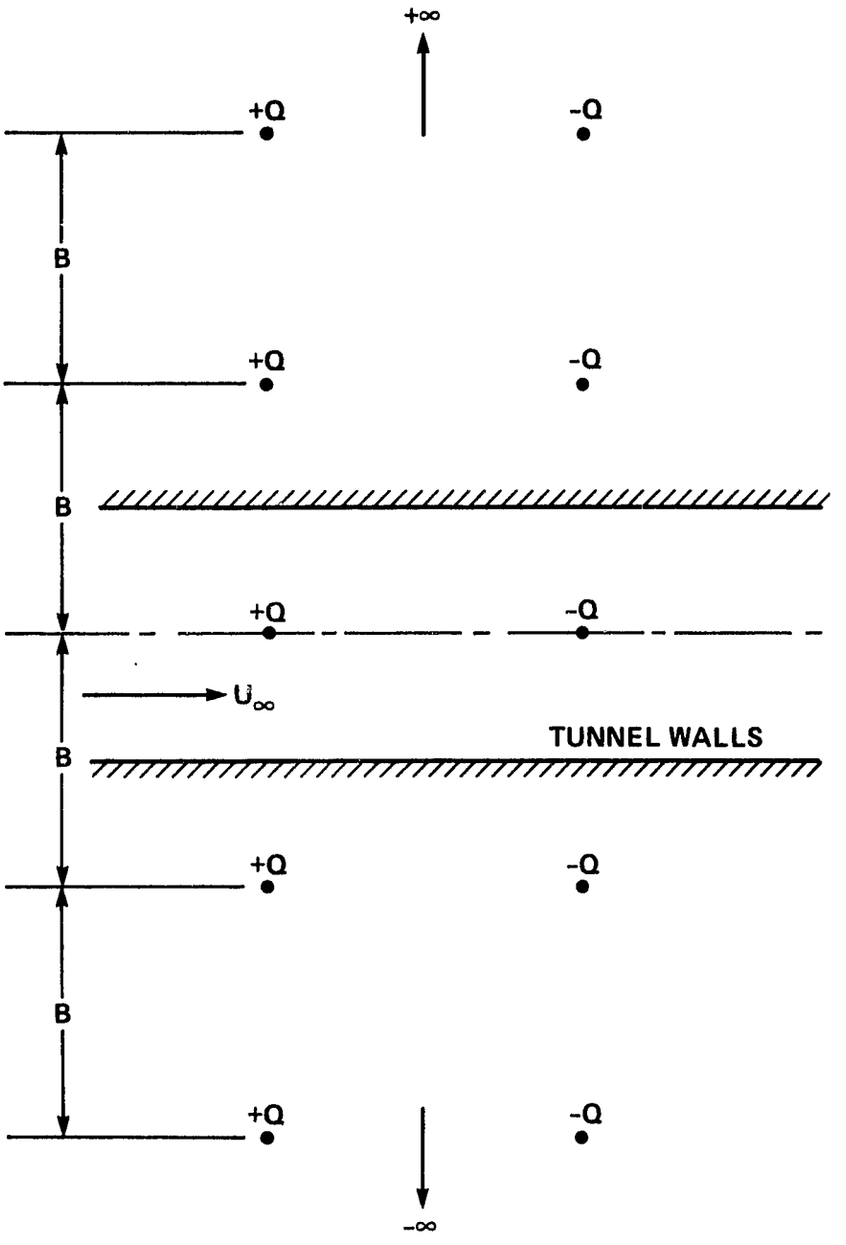

Figure 3. – Representation of wind tunnel walls by image systems

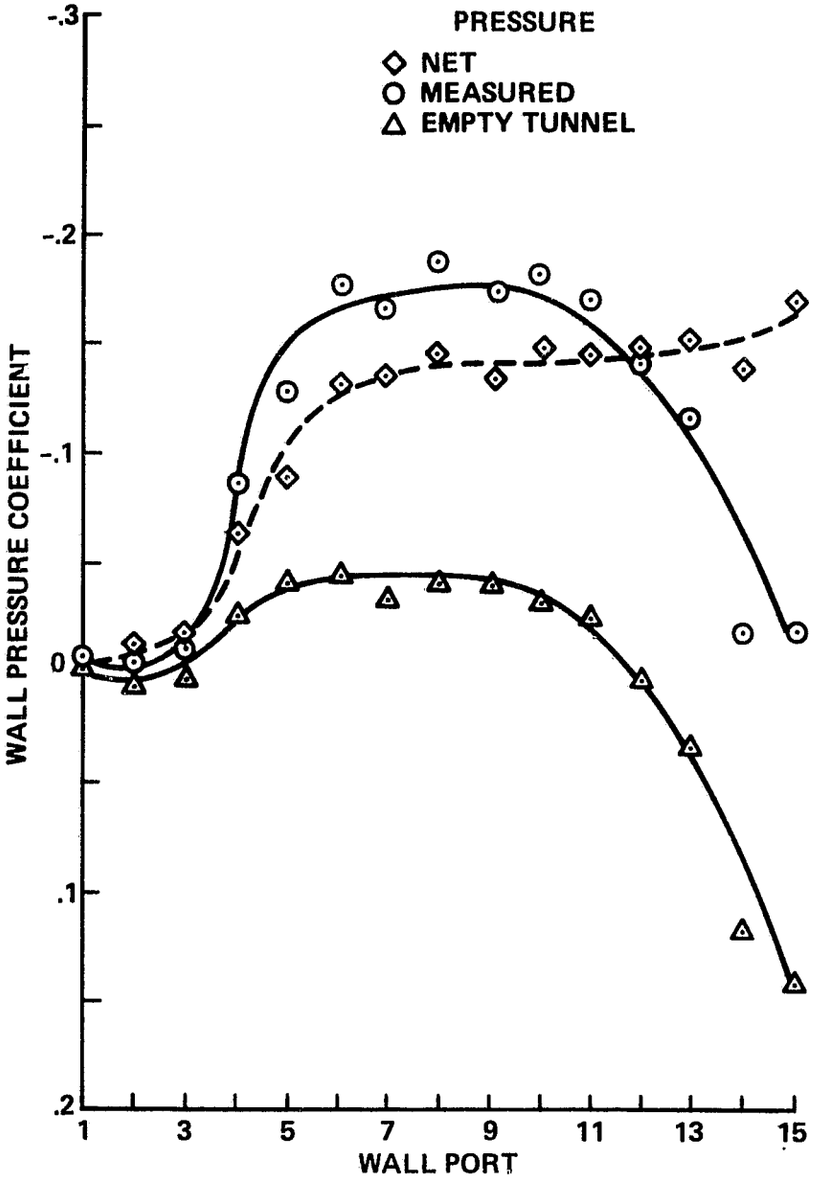

Figure 4. – Pressure distribution along wind tunnel walls for a model with triangular cross section; apex forward, $b = 0.10$

1. Report No.	2. Government Accession No.	3. Recipient's Catalog No.
NASA TM 86759		

4. Title and Subtitle	5. Report Date
ON BLOCKAGE CORRECTIONS FOR TWO-DIMENSIONAL TUNNEL TESTS USING THE WALL-PRESSURE SIGNATURE METHOD	March 1986
	6. Performing Organization Code

7. Author(s)	8. Performing Organization Report No.
S. R. Allmaras (Massachusetts Institute of Technology, Cambridge, MA)	A-86267
	10. Work Unit No.
9. Performing Organization Name and Address	
Ames Research Center Moffett Field, CA 94035	11. Contract or Grant No.
	13. Type of Report and Period Covered
12. Sponsoring Agency Name and Address	Technical Memorandum
National Aeronautics and Space Administration Washington, DC 20546	14. Sponsoring Agency Code 505-31-01-01

15. Supplementary Notes

Point of contact: W. J. McCroskey, Ames Research Center, M/S 202-1, Moffett Field, CA 94035 (415) 694-6428 or FTS 464-6428

16. Abstract

The Wall-Pressure Signature Method for correcting low-speed wind tunnel data to free-air conditions has been revised and improved for two-dimensional tests of bluff bodies. The method uses experimentally measured tunnel wall pressures to approximately reconstruct the flow field about the body with potential sources and sinks. With the use of these sources and sinks, the measured drag and tunnel dynamic pressure are corrected for blockage effects. Good agreement is obtained with simpler methods for cases in which the blockage corrections were about 10% of the nominal drag values.

17. Key Words (Suggested by Author(s))	18. Distribution Statement
Wind tunnel wall corrections Bluff-bodies airloads Wall-pressure signature	Unlimited Subject category - 02

19. Security Classif. (of this report)	20. Security Classif. (of this page)	21. No. of Pages	22. Price*
Unclassified	Unclassified	25	A02

*For sale by the National Technical Information Service, Springfield, Virginia 22161